Anal. Bioanal. Electrochem., Vol. 10, No. 6, 2018, 751-777

Analytical & Bioanalytical Electrochemistry

www.abechem.com

Full Paper

Extracts of Olive Inflorescence Flower Pre-Anthesis, at Anthesis and Grain Pollen as Eco-Friendly Corrosion Inhibitor for Steel in 1M HCl Medium

Driss Bouknana,[1,2,*] Belkheir Hammouti,[1,3] Shehdeh Jodeh,[4,*] Mohamed Sbaa and Hassane Lgaz[5,6]

[1]*LC2AME: Laboratory of Applied Analytical Chemistry, Materials and Environment; Faculty of Sciences, University Mohammed first, BP 4808, 60046 Oujda, Morocco*

[2]*COSTE: Center of the Oriental Science and Water Technologies; Faculty of Sciences, University Mohammed first, BP 4808, 60046 Oujda, Morocco*

[3]*Department of Chemistry, College of Science, King Saud University, B.O. 2455, Riyadh 11451, Saudi Arabia*

[4]*Department of Chemistry, An-Najah National University, P. O. Box 7, Nablus, State of Palestine*

[5]*Laboratory separation processes, Faculty of Science, University Ibn Tofail PO Box 242, Kenitra, Morocco*

[6]*Laboratory of Environmental Engineering and Biotechnology, ENSA, University Ibn Zohr, PO Box 1136, 80000 Agadir, Morocco*

*Corresponding Author, Tel.: (970) 599590498, (+212)670528010, Fax: (970) 9 2345982, +212 536 50 06 03

E-Mail: Bouknana.d@gmail.com ; sjodeh@najah.edu

Received: 4 November 2017 / Received in revised form: 5 January 2018 / Accepted: 14 March 2018 / Published online: 30 June 2018

Abstract- This work is devoted to examining the effectiveness of aqueous extracts of olive flower pre-anthesis, anthesis and grain pollen olive (Olea europaea L.) on corrosion of mild steel in 1 M HCl solution; The weight loss measurements, polarization curves and electrochemical impedance spectroscopy (EIS) infrared spectroscopy methods were

employed to evaluate corrosion rate and inhibition efficiency. The corrosion inhibition efficiencies of olive flower inflorescence pre-anthesis, anthesis and grain pollen are achieved 94%, 95.9%, and 94.8% in 1 M HCl, respectively. The inhibition efficiency is greatly reduced as the temperature is increased; the experimental results show that corrosion inhibition efficiency increases with concentration of the sample extract; polarization studies show that olive flower inflorescence pre-anthesis, anthesis and grain pollen extracts acts as a mixed inhibitor.

Keywords- Olive flower, Inhibitor, Corrosion, Steel, HCl solution

1. INTRODUCTION

The mild steel is one of the most metals used in industry, but, the use of the acid solutions in some industrial processes such as drilling operations in oil, gas exploration, pickling, and acid cleaning of steel structures, resulting a considerable corrosion of the metal[1–5].

The inhibitors are widely used in order to protect the metallic materials against degradation due to corrosion[6–10]. Organic compounds have become most accepted as effective corrosion inhibitors in various media in order to inhibit the corrosion reaction and reduce the corrosion rate by blocking the metal from coming into contact with the corrosive solution. A continuing effort has been made to develop a corrosion inhibitor that exhibits a greater inhibition effect at a low concentration in the corrosion medium as well as environment-friendly feature[11]. Most of the acid corrosion inhibitors are organic compounds containing electronegative atoms (such as O, N, S, and P etc.), unsaturated bonds and/or aromatic rings. The inhibitory performance of organic compounds is due to the adsorptive layer forming between the molecules with lone electron pair and/or π electrons and the surface metal atoms with unoccupied d-orbitals [12–17]. Currently, the research is oriented to the development of “green corrosion inhibitors” with good efficiency and low risk of environmental pollution[18].

Olive (Olea europaea.L) is the most extensively cultivated oleiferous tree species in the world, covering an area of 10 million of hectares [19]. The olive flower phenology is characterized by an annual cycle, including bud formation during the previous summer, dormancy during the cold period, and budburst in late winter, and flower structure development from budburst to flowering in spring [20]. The sexual reproduction of the olive tree is characterized by important phenomena such as alternate bearing [21], the pistil abortion [22], and the reproductive self and cross-incompatibility [23]. The olive floral buds are differentiating into inflorescences during winter, and floral bud differentiation begins in early February [24]. Differentiation takes place in late February and bloom in May when the formation of each flower part occurs in the inflorescence [25]. Some olive (Olea europaea.L) cultivars are almost completely self-incompatible, which means that the flowers are not fertilized by pollen of the same cultivar. The stigma was found to be receptive to pollen during the first four days after anthesis. Self-pollination resulted in germination of the pollen

grains on the stigma. Other cultivars are cross-incompatible, in which case flowers cannot or nearly not be fertilized by pollen from certain other cultivars. The degree of self-incompatibility varies among cultivars [26,27]. Differentiation of olive floral buds during winter is strictly related to flowering during spring and finally to fruit production during autumn-winter [28]. The following winter dormancy, the subsequent changes from axillary bud to blooming inflorescence constitute an extensive growth and development process which requires two to three months and includes the elongation and branching of the inflorescence axis and the formation and development of the individual flowers [22]. Floral initiation occurs by November [29], after which, the flower parts form in March. The inductive phase of flowering in the olive may take up to 8 months starting as early as July until about 6 weeks after full bloom, later in February, but initiation is not easily seen until 8 months later in February, Although floral initiation occurs in November, but the process of developing all the flower parts starts in March [30]. The development of reproductive phases in the olive is concentrated in a 5-6 weeks pre-anthesis period, from the end of April to the end of May [25]. Flowering of the olive tree occurs on paniculate and romonoecious inflorescences containing a mixture of perfect (hermaphrodite) flowers and functionally staminate (imperfect) flowers, Imperfect flowers are staminate, with the pistil either lacking or rudimentary, formed as a consequence by varying degrees of pistil abortion [31]. Perfect flowers, those with both pistillate and staminate parts; have a plump green pistil with a short, thick style and a large stigma. Only the hermaphroditic perfect flowers contain a pistil and thus the capability for forming a fruit. Staminate flowers have no pistil or only a tiny; yellow aborted one [32]. There is a cultivar-related tendency for producing imperfect flowers [33], as well as a noted influence of growing conditions such as moisture availability and nutritional status [34]. The proportion of perfect and staminate flowers depends on genetic, climatic conditions, and the level of fruit production in the previous year [23]; Therefore, it may vary from year to year, from tree to tree, from shoot to shoot, and from inflorescence to inflorescence [35]. Both perfect and staminate flowers produce viable pollen grains but only the perfect flowers set fruit [36]. The flowers are borne apically in an inflorescence, small, yellow-white, and inconspicuous [30]. The olive perfect flower consists of four fused green sepals, four white petals, two stamens each with a large yellow anther, and two carpels each with two ovules [32]. A mature olive (Olea europaea.L) tree produces about 500,000 flowers but only 1-2% of them set fruit that reach maturity [37]. At full bloom, flowers are delicately poised for pollination, 14 days after full bloom; most of the flowers destined to abscise have done so. By that time, about 494,000 flowers have abscised from a tree that started with 500,000 flowers [38]. Each inflorescence contains 15 - 30 flowers, depending on the cultivar [30]. The olive tree is allogamous (cross-fertilization in plants (opposed to autogamy), with a system of gametophytic self incompatibity [39], and anemophilous (Pollinated by wind dispersed pollen). Different aspects of the olive pollination biology have been well

documented abroad, such as pollen development [40], tapetum [41], pollen cell wall and aperture formation [42], maturation inside the anther [43] and pollen germination in vitro [44].

Embryo sac formation [45], ovary development [46], and pistil structure and composition [36] have also been described due to their significance for fruit development. Olive pollination is anemophilous and an adult olive tree can produce large amounts of pollen grains spread in the air during the flowering period [47]. Olive flowers bear large quantities of pollen and are wind pollinated [22]. However, olive pollen grains can traverse distances of more than 20-30 km, and the number of pollen grains significantly varied among the cultivars and between the two years [47]. Several studies in Mediterranean countries have shown a close association between the annual production of pollen and the consequent olive yield [48]. The olive (Olea europaea.L) pollen represents one of the main causes of allergy by inhalation [49].

Hence, in the present investigation an attempt has been made to use the olive flower pre-anthesis, anthesis and grain pollen extracts for the corrosion inhibition of mild steel in 1 M HCl. The investigations were made using of electrochemical and weight loss methods.

2. MATERIALS AND METHODES

2.1. Samples and Solutions

Fresh olive inflorescence flower pre-anthesis, anthesis and grain pollen were collected during harvesting in May 2014 from olive trees of the cultivar "*Picholine Moroccan (Olea europaea.L*" from an olive farm (Oujda), olive inflorescence flower pre-anthesis and anthesis samples were cleaned with tap water to eliminate ash of mud and washed with double-distilled water, and then dried in a well-ventilated shady place and subsequently stored in a dark room. The dried samples were then shredded into fine pieces.

Pictures of single flower buds are shown in (Fig.1): stages 1–6: developing flowers at pre-anthesis (26 to 3 days before anthesis), and stages 7–10: flowers at anthesis (0 to 3 days after anthesis).

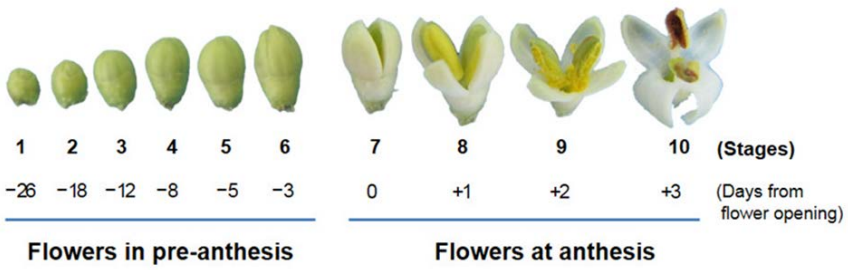

Fig. 1. Stages of olive flower development

The samples were collected at different stages, from the very early developmental stages

when the ovaries and stamens are developing (26, 18, 12, 8, 5 and 3 days before anthesis, respectively, which correspond to stages 1, 2, 3, 4, 5 and 6) , to anthesis and anther dehiscence, when the pollen grains interact with the pistils (0, 1, 2, 3 days after anthesis, which correspond to stages 7, 8, 9 and 10, respectively) [50].

2.2. Steel and HCl solution

The chemical composition of the steel used in this experiment is: 0.22% C, 0.79% Mn, 0.022% P, 0.030% S, 0.21% Si, 0.02% Ni; 0.030% Al, and the remainder is iron. Coupons of steel with dimensions (2, 2, 0.3 cm) and exposed surface area 4 cm^2 were used for weight loss measurements. For potentiostatic polarization experiments, a cylindrical rod of steel embedded in araldite with exposed surface area 0.4 cm^2 was used. The electrodes were polished with different grades of emery papers, degreased with acetone, and rinsed in distilled water before they were inserted into the test solution.

The aggressive solution of 1.0 M HCl was prepared by dilution of Analytical Reagents grade 37% HCl with distilled water.

All chemicals used for preparing the test solutions were of analytical grade and the experiments were carried out at room temperature, 25±1 °C.

2.3. Preparation olive flower pre-anthesis, anthesis and grain pollen extracts

Before the extraction, the samples were grinded using grinder with a sieve of 2.5 mm; 5 g of each sample was extracted three times with a solvent (methanol / water: 70/30: v / v) for 2 h in a water bath at 60 °C. The refluxed solution of each sample was filtered, and the filter liquor was evaporated to 100 ml of dark brown residue, and then degreased with hexane and extracted with separating funnel. The extract is filtered, and the collected liquid is used to prepare the desired concentrations by dilution.

2.4. Infrared drying experiments

The milled samples of olive flower pre-anthesis, anthesis and grain pollen were characterized by Fourier transform infrared (FTIR) spectroscopy. FTIR spectra was recorded in an AVATAR-FTIR-360 spectrophotometer (Thermo Nicolet Company, USA), which extended from 4000 to 400 cm^{-1}, using the Potassium bromide (KBr) disk technique.

2.5. Weight loss measurements

Weight loss tests were conducted under total immersion in 50 ml of non-deaerated HCl solutions without and with three inhibitors tested (olive flower inflorescence pre-anthesis, anthesis and grain pollen), the steel coupons were left hanging in the test solution for 6 h (immersion time) at 308 K before their loss of weight was recorded, then the specimens were

taken out, washed with bristle brush under running water to remove the corrosion product, dried with a hot air stream, and reweighed accurately. The corrosion rate was calculated, in milligrams per square centimeter per hour ($mg.cm^{-2}.h^{-1}$), on the basis of the apparent surface area. In order to investigate the effects of temperature on the inhibitor performance, the tests were carried out in a temperature range 313-338 K with 1 h immersion time for the weight loss. The mean weight loss of all parallel steel was obtained, and then corrosion rate (W) and the percentage inhibition efficiency (% IE_w) of the extracts was calculated using the following equation (1).

$$IE_w\% = 100 \times \left(\frac{W_{Corr} - W^{o}_{Corr}}{W_{Corr}} \right) \quad (1)$$

Where W_{corr} and W°_{corr} are corrosion rates of the mild steel without and with different samples extracts, respectively.

2.6. Electrochemical measurements

The electrochemical study was carried out using a potentiostat PGZ100 piloted by Volta master software, this potentiostat is connected to a cell with three-electrodes with a platinum counter electrode (CE), a saturated calomel electrode (SCE) coupled to a fine Luggin capillary as the reference electrode (RE) and a working electrode (WE); the surface area exposed to the electrolyte is 1 cm^2.

Potentiodynamic polarization curves were plotted at a polarization scan rate of 1 mV/s; before all experiments, the potential was stabilized at free potential during 30 min, the polarization curves are obtained from -800 mV to -200 mV at 308 K. The solution test has been achieved after de-aerated by bubbling nitrogen; gas bubbling is maintained prior and through the experiments. The electrochemical impedance spectroscopy (EIS) is a reliable and powerful technique to study the electric properties of the electrochemical systems. It is widely spread in various fields of research such as corrosion [51–55], characterization of the thin layers, and kinetics of electrode and batteries [56–61].

The principle of the realized electrochemical sensor bases on the measure of the impedance of an electrochemical cell by the technique of spectroscopy of impedance, this technique allows controlling the process of charges transfer in the interface electrode/electrolyte. Indeed, a potential imposed with a sinusoidal disturbance of low amplitude, between the reference electrode and the indicator electrode, allows the measure of a current, of the same shape, generated between the indicator electrode and the auxiliary electrode.

The data in Tafel region have been processed for evaluating the corrosion kinetic parameters by plotting the polarization curves. In a large domain of the potential, the linear

Tafel segments of the cathodic curves were extrapolated to the corresponding corrosion potentials to obtain the corrosion current values. The inhibition efficiency (IE_{pol}) was evaluated using the relationship equation (2).

$$IEpol\% = 100 \times \left(\frac{I^{o}_{Corr} - I_{Corr}}{I^{o}_{Corr}} \right) \quad (2)$$

To determine the impedance parameters of the C38 steel specimens in acidic solution, the measured impedance data were analyzed using Z_{view} program based upon an electric equivalent circuit [62,63]. The charge transfer-resistance (R_t) values were calculated from the difference in impedance at low and high frequencies [64–68]; The double layer capacitance (C_{dl}) was obtained at the frequency f_{max} at which the imaginary component of the impedance is maximal (Z_i max) by equation (3).

$$C_{dl} = 1/(2\pi.f_{max}.R_t) \quad (3)$$

The inhibition efficiency of the inhibitors has been determined from equation (4), where R_{inh} and R°_{inh} are the charge transfer resistance values in the absence and in the presence of the inhibitors, respectively.

$$IE_{imp}\% = 100 \times \left(\frac{R_{inh} - R^{o}_{inh}}{R_{inh}} \right) \quad (4)$$

In order to get good reproducibility, all the experiments were carried out in triplicate.

2.7. SEM

The analysis of steel sample in the acidic solutions with and without the optimum concentration of inhibitors was performed after 6 h of immersion in uninhibited and inhibited solution using SEM. SEM (Hitachi TM-1000) with an accelerating voltage of 15 kV was used for the experiments.

3. RESULTS AND DISCUSSIONS

3.1. Weight loss measurements

In order to assess of plant extract inhibitors will be effectively inhibiting the corrosion of metals in acid medium, the weight loss method of monitoring corrosion rate and inhibition efficiency is useful because of its simple application and high reliability [69]. The data of Table.1 represent the results obtained from weight loss experiments: the corrosion rate (W) and the inhibition efficiency percentage (% IE_w) of mild steel coupons in 1M HCl at 308 K after 6 h of immersion period in the presence of different concentrations of olive flower pre-

anthesis, anthesis and grain pollen.

Table.1. Gravimetric results of steel in 1 M HCl with and without addition various concentrations of inhibitors at 308 K

Inhibitor	**Concentration mg/L**	**W (mg $cm^{-2}.h^{-1}$)**	**IE%**
Blank	1 M	0.8685	****
OFIPAE	4.00E-03	0.228610663	73.68
	8.00E-03	0.199879975	76.99
	1.20E-02	0.198737648	77.12
	1.60E-02	0.170706312	80.34
	2.00E-02	0.150778155	82.64
OFIAE	4.00E-03	0.200514216	76.91
	8.00E-03	0.156244498	82.01
	1.20E-02	0.140839918	83.78
	1.60E-02	0.13429889	84.54
	2.00E-02	0.117917449	86.42
OGPE	5.00E-05	0.238245928	72.57
	1.00E-04	0.206490461	76.22
	1.50E-04	0.183393896	78.88
	2.00E-04	0.164350113	81.08
	2.50E-04	0.140148031	83.86

Inspection of the Table.1 reveals that the rate of carbon steel corrosion is greatly reduced upon the addition of the selected three inhibitors of olive samples extracts (olive flower pre-anthesis, anthesis and grain pollen) and decreases with the inhibitor concentration due to the fact that the adsorption coverage increases, which shields the steel surface efficiently from the acid solution; in acidic media; the corrosion rate decreases sharply with an increase in samples concentrations, the corrosion inhibition enhances with the inhibitor concentration.

At any given inhibitor concentration, despite the difference in concentrations between the olives flowers inflorescence pre-anthesis, anthesis and olive pollen grain, the corrosion rate follows the order: W (OFIA)<W (OGP)<W (OFIPA), which indicates that (OFIA) exhibits the best inhibitive performance among these additives. Clearly, the inhibition efficiency increases with an increase in the inhibitor concentration, it reaches 82.64%, 86.42% at 2×10^{-2} mg/L for olive flower inflorescence pre-anthesis and anthesis, respectively, and 83.86% at 2.5×10^{-4} mg /L for grain pollen of the added extracts. This behavior is due to the fact that the adsorption amount and coverage of inhibitor on steel surface increases with the inhibitor concentration. The inhibitive action of olive flowers extracts acts as a barrier between the steel surface and the aggressive solution, leading to a decrease in the corrosion rate.

It could be concluded that the inhibition efficiency of inhibitors follows the general order: *%IE* (OFIAE)>*%IE* (OGPE) >*%IE* (OFIPAE). This result implies that the crude extract of olive flower inflorescence anthesis exhibits better inhibition performance than its major components.

The surface morphologies of steel surfaces exposed to 1 M HCl solutions in the absence and presence of inhibitors after 6 h of immersion were examined using SEM. The changes that occurred in the steel samples are shown in Fig. 2(A–D). Fig. 2(A) shows the steel surface in 1 M HCl, which is severely corroded due to attack of acid on mild steel. Fig. 2(B-D) shows the steel surface in 1 M HCl containing optimum concentration of inhibitors. However, in presence of inhibitors, the surface morphology remarkably improved due to the adsorption of inhibitors on metal surface protecting it from acid corrosion.

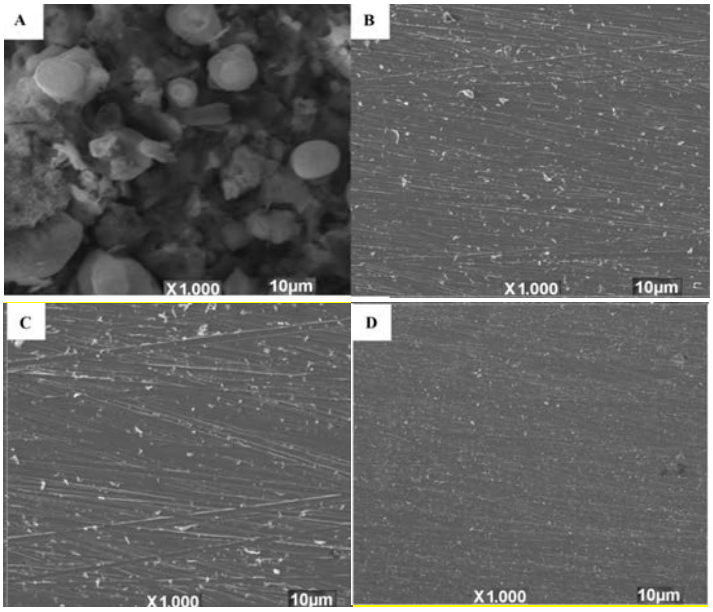

Fig. 2. SEM photos of steel plates after 6 hours of immersion in (A) corrosive solution, 1 M HCl and in presence of: (B) Extracts of Olive Inflorescence Flower Pre-Anthesis; (C) Anthesis; and (D) the pollen grain

3.2. Polarization studies

3.2.1. Potentiodynamic polarization curves

The inhibition of samples extracts on mild steel specimens immersed in 1 M HCl was further studied by measuring the change in the cathodic and anodic behaviors of the specimens which correspond to hydrogen reduction and metal oxidation.

The cathodic and anodic potentiodynamic polarization curves of C-steel in 1 M HCl. solution without and with different concentrations of samples extracts were recorded at a scanning rate of 5 mV/s at 35 °C (immersion time is 30 h) are represented in (Fig. 3).

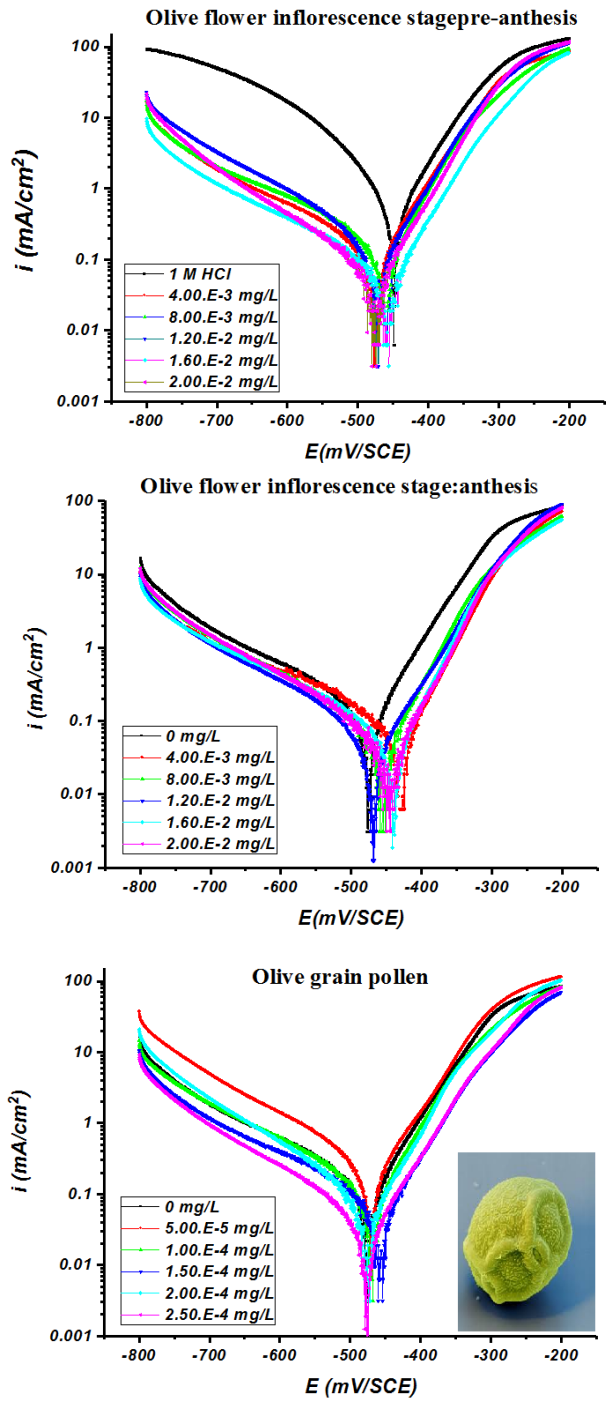

Fig. 3. Typical polarisation curves of steel in 1 M HCl for various concentrations of Olive flower developmental stages grouped into two periods: pre-anthesis and anthesis and olive grain pollen at 308 K

Inspection of the (Fig. 3) reveals that the polarization curves are shifted toward more negative potentials and less current density upon addition of olive flowers extracts or olive grain pollen extract, this phenomenon corresponds to a decrease in the corrosion rate which can be explained by the shift of the cathodic and anodic Tafel slopes; it is also noticed that

there was a clear shift for both anodic and cathodic parts for the sweeps at the various test concentrations; the shift range in the cathodic Tafel slopes of the tests is more noticeable than the shift range in the anodic Tafel slopes, this may indicate that the decrease of the oxidation rate of the metal with higher extract concentrations corresponds to the relative drop in the corrosion rate. The extract adsorption on the metal surface is causing the decrease in the metal dissolution at a relatively more noticeable/ higher rate while affecting the hydrogen reduction to a lesser extent; the shifts in both anodic and cathodic curves indicate that the olive flower extract is a mixed inhibitor with significant cathodic efficiency for olive grain pollen, but, perfect mixed inhibitor for the others sample: olive flower inflorescence pre anthesis and anthesis.

The Potentiodynamic polarization parameters including corrosion current densities (I_{corr}), corrosion potential (E_{corr}), cathodic Tafel slope (β_c), anodic Tafel slope (β_a), and inhibition efficiency ($\%IE_{pol}$) are presented in Table.2.

Table 2. Polarization parameters for steel in 1 M HCl acid at different types of the olive grain pollen, Olive flower inflorescence pre-anthesis and anthesis at 308 K at the various concentrations.

Samples	**Concentration mg/L**	**E_{corr}** (mV/SEC)	**β_a** (mV/dec)	**$-\beta_c$** (mV/dec)	**I_{corr}** (mA/cm2)	**IE_{pol} (%)**
Blank	1 M	-450	63	-87.4	0.3765	*
OFIPAE	4.00E-03	-476.4	64.9	-153.3	0.0843	77.6
	8.00E-03	-461.6	56.9	-155.5	0.079	79
	1.20E-02	-472.8	60.3	-126.4	0.0677	82
	1.60E-02	-459.1	61.3	-137.3	0.0401	89.3
	2.00E-02	-474.6	57	-136.7	0.034	91
OFIAE	4.00E-03	-430.8	53.8	-123.6	0.0366	90.3
	8.00E-03	-453.8	55	-134.7	0.0341	90.9
	1.20E-02	-469.6	68	-136.9	0.0301	92
	1.60E-02	-440	51.2	-139.6	0.0286	92.4
	2.00E-02	-449.4	51.3	-112.3	0.0153	95.9
OGPE	5.00E-05	-471.3	64.1	-130.6	0.111	70.5
	1.00E-04	-471.2	59.3	-135.6	0.0584	84.5
	1.50E-04	-457.1	62.1	-144.5	0.0394	89.5
	2.00E-04	-476.1	55.7	-121.7	0.032	91.5
	2.50E-04	-476.3	64.1	-127.2	0.0225	94

Inspection of the data of the Table 2 revealed that the corrosion potential shifts to more negative values with increased concentrations of olive extracts; moreover, the corrosion current density decreases markedly on addition of the extract.

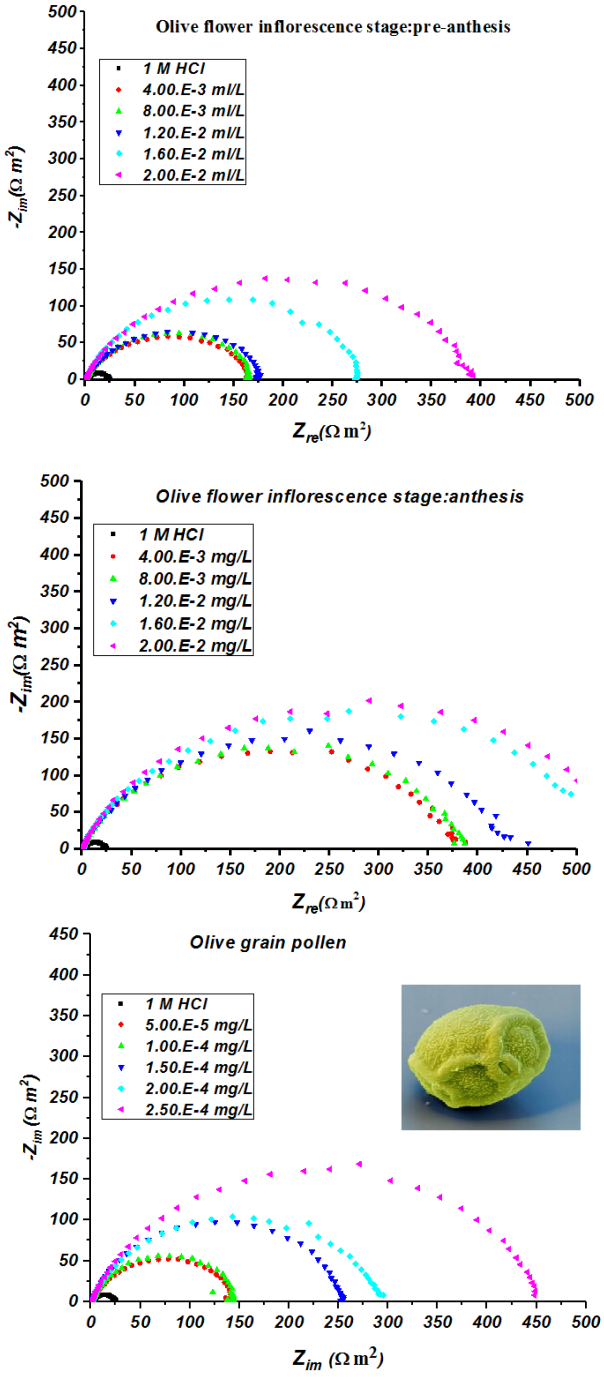

Fig. 4. Nyquist diagrams for steel electrode with and without Olive flower developmental stages grouped into two periods: pre-anthesis and anthesis and olive grain pollen after 30 min of immersion in 1 M HCl for various concentrations

I_{corr} decreases considerably in the presence of inhibitor in acid, and decreases with the increase of inhibitor concentration. The inhibition efficiency increases with increasing extract concentration for reaches up 91%, 95.9% and 94% for olive flower inflorescence pre-anthesis, anthesis and grain pollen respectively. This result suggests that the presence of the extracts affect the anodic dissolution of steel as well as the cathodic reduction of hydrogen

ions. Therefore, it could be concluded that the molecules of extract absorb onto both anodic and cathodic sites of the steel surface. This behavior indicates that the extracts act as a mixed inhibitor.

3.2.2. Electrochemical impedance spectroscopy (EIS)

Electrochemical impedance spectroscopy (EIS) was used to obtain information about the kinetics and mechanism of the mild steel corrosion inhibition by the olive extracts at 308K.

Table 3. Impedance parameters of steel in acid at various samples of the olive grain pollen, Olive flower inflorescence pre-anthesis and Olive flower inflorescence anthesis

Samples	**Concentration mg/L**	**R_{pol} ($\Omega.cm^2$)**	**f_{max} (Hz)**	**C_{dl} (nF/cm^2)**	**IE_{pol}% Polarisation**	**IE_{imp}% Impedance (EIS)**	**IE_w% gravimetric**
Blank HCl	1 M	23.45	125	4602.06	-	-	-
OFIPAE	4.00E-03	164.3	15.823	4081.56	77.6	85.7	73.7
	8.00E-03	165.7	11.4071	2967.55	79	85.8	77
	1.20×10^{-2}	189.5	20	5950.3	82	87.6	77.1
	1.60×10^{-2}	276.1	7.9365	3440.29	89.3	91.5	80.3
	2.00×10^{-2}	392.2	7.9365	4886.93	91	94	82.6
OFIAE	4.00×10^{-3}	381	6.3291	3785.88	90.3	93.8	76.9
	8.00×10^{-3}	386.4	4	2426.59	90.9	93.9	82
	1.20×10^{-2}	434.4	4	2728.03	92	94.6	83.8
	1.60×10^{-2}	547	4	3435.16	92.4	95.7	84.5
	2.00×10^{-2}	553.2	4	3474.1	95.9	95.8	86.4
OGPE	5.00×10^{-5}	138.3	20	4342.62	70.5	83	72.6
	1.00×10^{-4}	141.4	15.823	3512.67	84.5	83.4	76.2
	1.50×10^{-4}	253.6	10	3981.52	89.5	90.8	78.9
	2.00×10^{-4}	293.3	10	4604.81	91.5	92	81.1
	2.50×10^{-4}	453.4	4	2847.35	94	94.8	83.9

(Fig.4) shows the Nyquist diagrams for steel in 1 M HCl at 308 K with and without olive extracts, these diagrams have similar shape throughout all tested conditions, indicating that there is almost no change in the corrosion mechanism occurs due to the inhibitor addition. The impedance spectra exhibit one single capacitive loop, which indicates that the corrosion

of steel is mainly controlled by the charge transfer process [70]. In HCl acid, with respect to blank solution, the shape is maintained throughout all tested concentrations, indicating that there is almost no change in the corrosion mechanism occurs regardless of the inhibitor addition [71]. It is noted that the capacitive loop in acid is not perfect semicircle which can be attributed to the frequency dispersion effect as a result of the roughness and inhomogeneous of electrode surface [72].

Furthermore, the diameter of the capacitive loop in the presence of olive extracts is larger than that in blank solution, and the diameter of Nyquist plots increased upon increasing the concentration of olive flower extracts which resulted in strengthening the inhibitive film, this indicates that the impedance of inhibited substrate increases with the inhibitor concentration, and leads to good inhibitive performance [73]. The kinetic parameters derived from the Nyquist plots and the percentages of inhibition efficiency are given in Table 3. As the concentration of inhibitor increased, the capacitance (C_{dI}) decreased and polarizing resistance (R_{ct}) increased. The results of the inhibition efficiencies obtained from weight loss measurements *(%IE$_w$)*, potentiodynamic polarization curves *(%IE$_{pol}$)* and EIS *(%IE$_{imp}$)* are in good reasonably agreement.

The electrochemical parameters: R_p: charge transfer resistance, (C_{dI}): Double layer capacitance, f_{max}: represents the frequency at which imaginary value reaches a maximum on the Nyquist plot and %E: efficiency percentage. The EIS results of these capacitive loops are simulated by the equivalent circuit shown in (Fig. 4) to pure electric models that could verify or rule out mechanistic models and enable the calculation of numerical values corresponding to the physical and/or chemical properties of the electrochemical system under investigation [74].

The circuit employed allows the identification of both solution resistance (Rs) and charge transfer resistance (R_t). It is worth mentioning that the double layer capacitance (C_{dl}) value is affected by imperfections of the surface, and that this effect is simulated via a constant phase element (CPE) [75]. The CPE is composed of a component Qdl and a coefficient a. The parameter "a" quantifies different physical phenomena like surface in homogeneousness resulting from surface roughness, inhibitor adsorption, porous layer formation; therefore, the capacitance is deduced from the following equation (5) [76]:

$$Cdl = Qdl * \left(2\pi f_{\max}\right)^{a-1} \quad (5)$$

Where f_{max} represents the frequency at which imaginary value reaches a maximum on the Nyquist plot. The electrochemical parameters of R_t, C_{dl} and IE_{imp} are calculated by $ZS_{imp}W_{in}$ software and presented in Table 3. Clearly, R_{pol} increases prominently while C_{dl} reduces with the concentration of olive flower extracts in acid. A large charge transfer resistance is associated with a slower corroding system. In contrast, better protection provided by an

inhibitor can be associated with a decrease in capacitance of the metal according to Helmholtz model (Fig.5) [77].

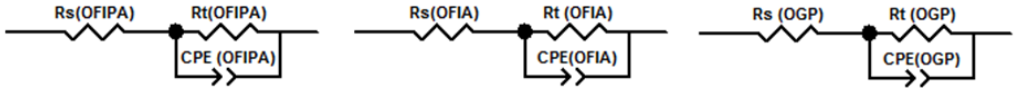

Fig. 5. Equivalent circuit used to fit the capacitive loop of olive flower inflorescence pre-anthesis, anthesis and olive grain pollen

3.3. Effect of the temperature

3.3.1. Weight loss, corrosion rates and inhibition efficiency

The composition of the medium and its temperature are essential parameters affecting the corrosion rate of metal and modifies the adsorption of inhibitor on electrode surface, the effect of the absence and presence of olive flower extracts tested at different concentration during 1 h of immersion on the corrosion of steel in 1 M HCl solution was studied by using weight-loss at different temperatures from 313 K to 343 K, The inhibition efficiency E_w(%) is calculated at a various concentrations as follows equation (6). The corresponding data are shown in Table 4.

$$E\% = 100 \times \left(\frac{W_{Corr} - W^{o}{}_{Corr}}{W_{Corr}} \right) \quad (6)$$

Where both W_{corr} and W°_{corr} are the corrosion rate of steel in 1M HCl in the absence and presence of olive flower extracts, respectively.

Table 4. Effect of temperature on the corrosion rate of steel at various samples of three samples in 1h of immersion at the different concentrations

Inhibitor	**T, (K)**	**Concentration mg/L**	**W (mg cm^{-2} h^{-1})**	**IE$_w$%**
Blank	313	1M	1.8669	-
	323	1M	2.4991	-
	333	1M	3.0812	-
	343	1M	4.9746	-
Olive flower inflorescence Pre-anthesis extract (OFIPAE)	313	4.00×10^{-3}	0.527	71.75
		8.00×10^{-3}	0.492	73.61
		1.20×10^{-2}	0.433	76.79
		1.60×10^{-2}	0.403	78.39
		2.00×10^{-2}	0.365	80.43
	323	4.00×10^{-3}	0.832	66.71

		8.00×10^{-3}	0.678	72.84
		1.20×10^{-2}	0.669	73.21
		1.60×10^{-2}	0.604	75.8
		2.00×10^{-2}	0.527	78.89
	333	4.00×10^{-3}	1.608	47.8
		8.00×10^{-3}	1.389	54.92
		1.20×10^{-2}	1.332	56.75
		1.60×10^{-2}	1.201	61.01
		2.00×10^{-2}	1.083	64.85
	343	4.00×10^{-3}	2.825	43.19
		8.00×10^{-3}	2.523	49.28
		1.20×10^{-3}	2.417	51.41
		1.60×10^{-2}	2.324	53.28
		2.00×10^{-2}	2.281	54.13
Olive flower inflorescence anthesis extract(OFIAE)	313	4.00×10^{-3}	0.514	72.42
		8.00×10^{-3}	0.424	77.27
		1.20×10^{-2}	0.318	82.96
		1.60×10^{-2}	0.302	83.77
		2.00×10^{-2}	0.290	84.45
	323	4.00×10^{-3}	0.794	68.21
		8.00×10^{-3}	0.608	75.65
		1.20×10^{-2}	0.554	77.8
		1.60×10^{-2}	0.481	80.75
		2.00×10^{-2}	0.456	81.73
	333	4.00×10^{-3}	1.336	56.64
		8.00×10^{-3}	1.225	60.23
		1.20×10^{-2}	1.163	62.24
		1.60×10^{-2}	1.007	67.29
		2.00×10^{-2}	0.981	68.14
	343	4.00×10^{-3}	2.853	42.64
		8.00×10^{-3}	2.491	49.91
		1.20×10^{-2}	2.411	51.53
		1.60×10^{-2}	2.373	52.28
		2.00×10^{-2}	2.206	55.64
Olive grain pollen extract(OGPE)	313	5.00×10^{-5}	0.538	71.14
		1.00×10^{-4}	0.455	75.6
		1.50×10^{-4}	0.412	77.92
		2.00×10^{-4}	0.358	80.8
		2.50×10^{-4}	0.323	82.69
	323	5.00×10^{-5}	0.991	60.31
		1.00×10^{-4}	0.761	69.52
		1.50×10^{-4}	0.656	73.71
		2.00×10^{-4}	0.606	75.74
		2.50×10^{-4}	0.561	77.52
	333	5.00×10^{-5}	1.570	49.04
		1.00×10^{-4}	1.332	56.76
		1.50×10^{-4}	1.266	58.89
		2.00×10^{-4}	1.223	60.3

		2.50×10^{-4}	1.035	66.39
	343	5.00×10^{-5}	2.974	40.2
		1.00×10^{-4}	2.656	46.59
		1.50×10^{-4}	2.447	50.81
		2.00×10^{-4}	2.410	51.54
		2.50×10^{-4}	1.693	65.95

The inhibition efficiency of the olive extract decreases markedly with increasing temperature, which can be attributed to that the higher temperatures might cause desorption of inhibitor molecule from metal surface, this result supports the idea that the adsorption of components olive extracts onto the steel surface is physical in nature, thus, as the temperature increases, the number of adsorbed molecules decreases, leading to a decrease in the inhibition efficiency. We summarize the results of the sets of the speed variations of the corrosion and efficiency inhibition of the corrosion according to the concentration and temperature in the following Table.5.

3.3.2. Thermodynamic parameters

To calculate activation thermodynamic parameters of the corrosion reaction at various temperatures (313–343 K) in the presence and absence of olive extracts at 1 h of immersion, such as the energy E_a, the entropy ΔS°_{ads} and the enthalpy ΔH°_{ads} of activation, Arrhenius equations (7 and 9) and its alternative formulation called transition state equations (8 and 10) were used.

$$W = K\exp\left(-\frac{E_a}{RT}\right) \quad (7)$$

$$\log(w) = -\frac{E_a}{RT} + k \quad (8)$$

$$W = \frac{RT}{Nh}\exp\left(\frac{\Delta S_a^o}{R}\right)\exp\left(-\frac{\Delta H_a^o}{RT}\right) \quad (9)$$

$$\log(W/T) = \left[\left(\log(\frac{R}{Nh}) + \frac{\Delta S_a^o}{R}\right)\right] - \frac{\Delta H_a^o}{RT} \quad (10)$$

Where T is the absolute temperature, K is a constant, Ea is the apparent activation corrosion energy, R is the universal gas constant, A is the Arrhenius pre-exponential factor, h is Plank's constant, N is Avogadro's number, ΔS°_{ads} is the entropy of activation and ΔH°_{ads} is the enthalpy of activation.

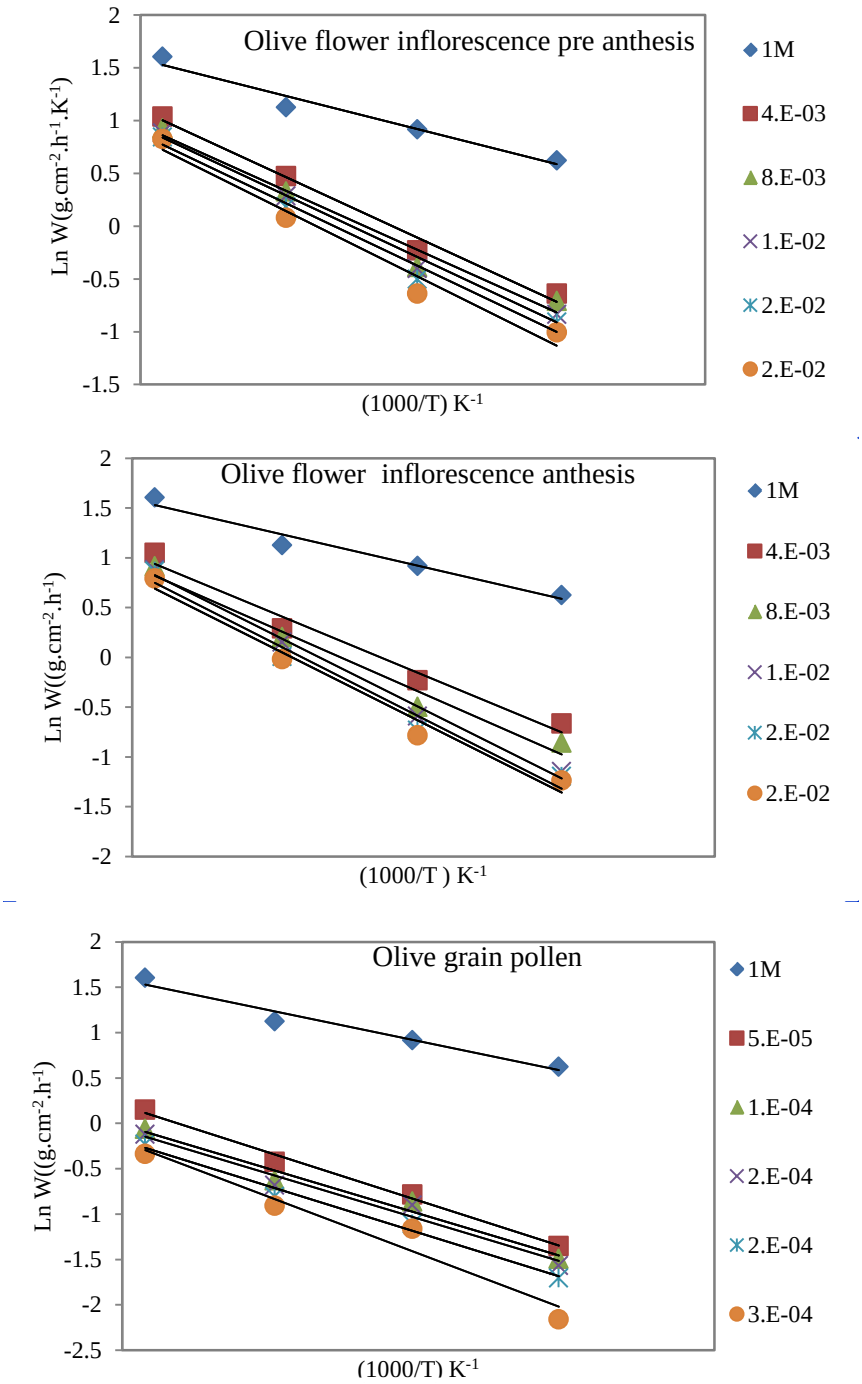

Fig. 6. Typical Arrhenius plots for Ln(W) *vs.* (1000/T) for steel in 1 M HCl at different temperatures and concentrations of Olive flower developmental stages grouped into two periods: pre-anthesis and anthesis and olive grain pollen

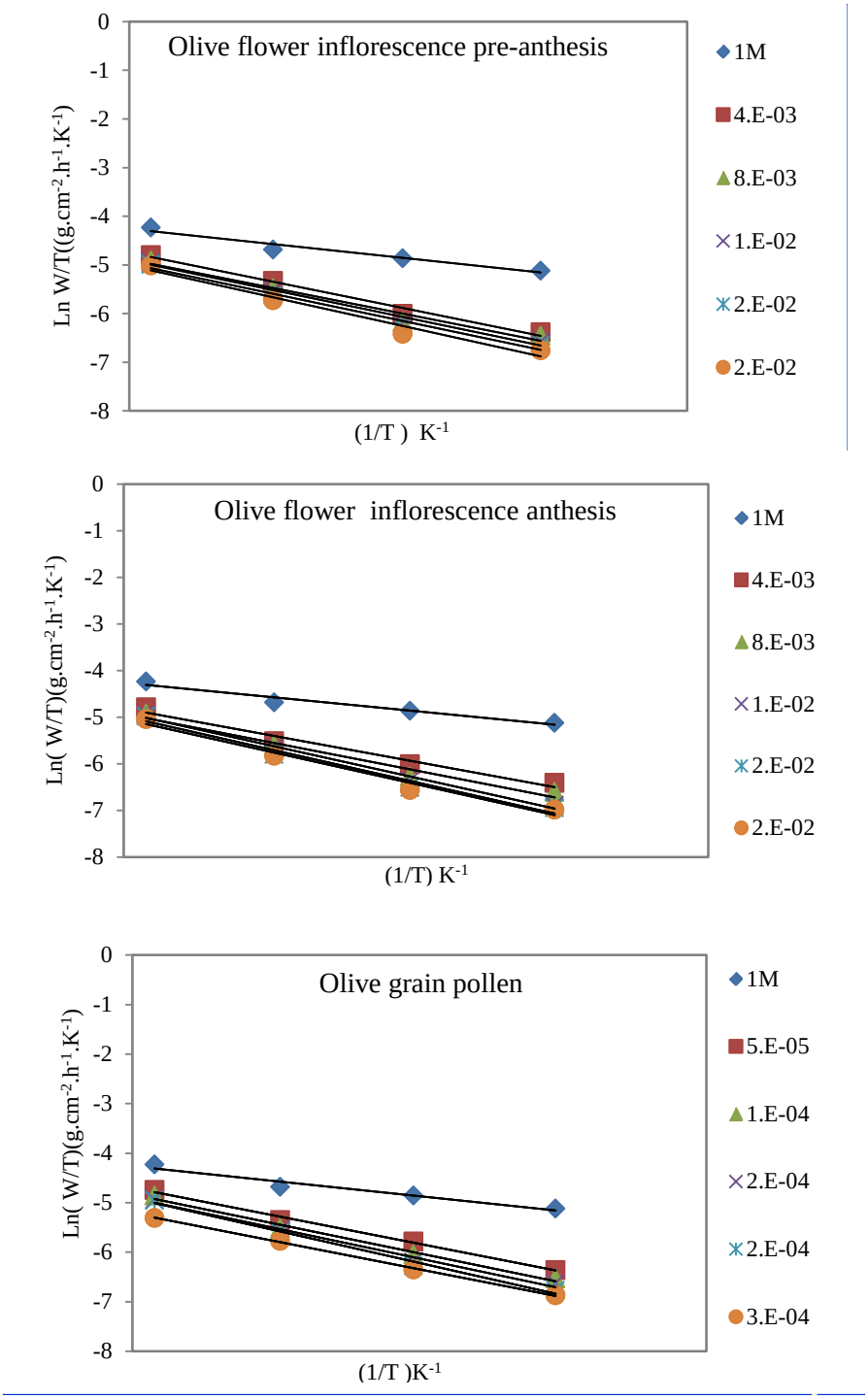

Fig. 7. The relation between Ln (W / T) *vs.* 1/T for steel at different temperatures and concentrations of Olive flower developmental stages grouped into two periods: pre-anthesis, anthesis and olive grain pollen

Table 5. Activation parameters of the dissolution of mild steel in 1 M HCl in the absence and presence of different concentrations of olive flower inflorescence pre anthesis, anthesis and grain pollen at various temperatures from 313 to 343 K

Samples	**Concentration mg/L**	**E_a (kJ/mol)**	**ΔH°_a (kJ/mol)**	**E_a-ΔH°_a (kJ/mol)**
Blank	1M	28	25.3	2.7
Olive flower inflorescence pre anthesis extract	4.00×10^{-3}	51.1	48.4	2.7
	8.00×10^{-3}	49.9	47.2	2.7
	1.20×10^{-2}	52.1	49.4	2.7
	1.60×10^{-2}	52.8	50.1	2.7
	2.00×10^{-2}	55.2	52.5	2.7
Olive flower inflorescence anthesis extract	4.00×10^{-3}	50.3	47.6	2.7
	8.00×10^{-3}	53.4	50.7	2.7
	1.20×10^{-2}	61.5	58.8	2.7
	1.60×10^{-2}	60.7	58	2.7
	2.00×10^{-2}	60.9	58.2	2.7
Olive grain pollen extract	5.00×10^{-5}	43.5	40.8	2.7
	1.00×10^{-4}	40.5	37.8	2.7
	1.50×10^{-4}	40.7	38	2.7
	2.00×10^{-4}	42.1	39.4	2.7
	2.50×10^{-4}	51.4	48.7	2.7

The inhibition efficiency decreases with the increase in temperature and the activation energy increases with increase inhibitor concentrations. This behavior is an indication of the formation of an adsorption film of physical electrostatic nature [78]. The obtained results suggest that olive flowers extracts inhibit the corrosion reaction by increasing its activation energy. This could be done by adsorption onto the steel surface, making a barrier to mass and charge transfer. However, such types of inhibitors perform good inhibition at ordinary temperature, with considerable loss in inhibition efficiency at elevated temperatures.

The linear regressions between Ln w and 1000/T were calculated, and the parameters given in the Table.6 and the (Fig. 6-7) shows the Arrhenius straight lines of Ln w *vs*. 1000/T for the blank and different inhibitors. All the linear regression coefficients (r) are very close to 1, which indicates that the linear relationship between Ln w and 1000/T is good. Kinetic parameter of apparent activation energy (E_a) is important to study the inhibitive mechanism. Compared with uninhibited solution, the increase of (E_a) in inhibited solution may be interpreted as the physical adsorption [79].

Inspection of the Table.6 reveals that the value of E_a in the presence of any inhibitor is higher than that in the uninhibited acid solution, which indicates that the adsorption of inhibitor is mainly the physical adsorption, while the weak chemical bonding between the inhibitor molecules and the steel surface would also occur [80].

3.4. Fourier transforms infrared (FTIR) spectroscopy of (olive flower inflorescence pre-anthesis, anthesis and grain pollen)

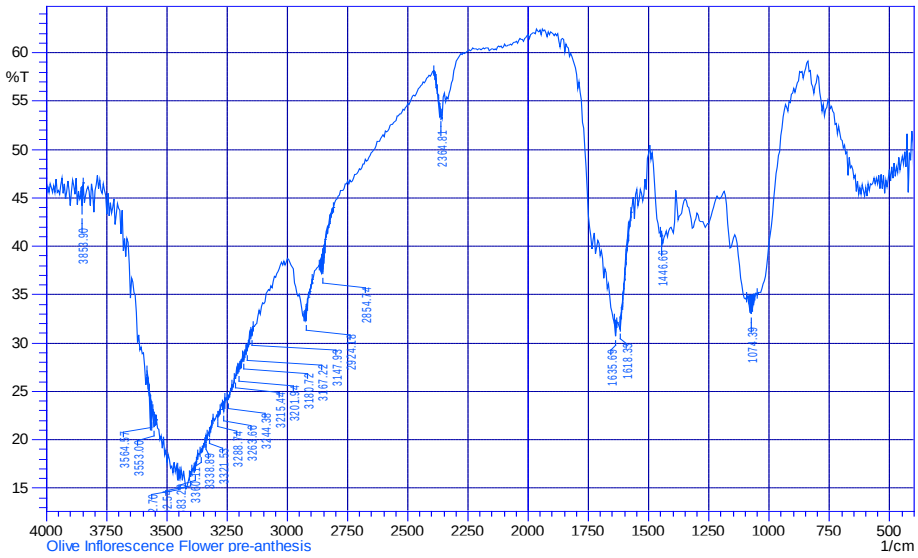

Fig. 8. Fourier transforms infrared (FTIR) spectroscopy of olive inflorescence flower pre-anthesis

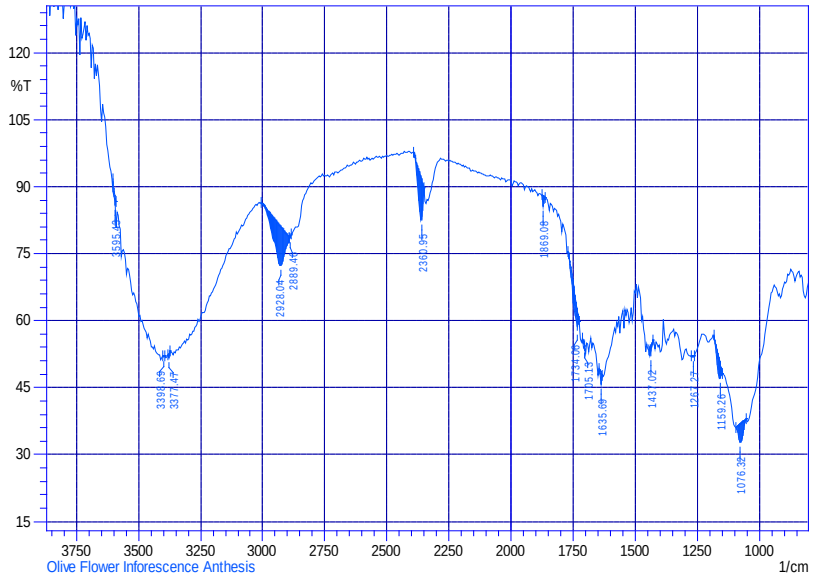

Fig. 9. Fourier transforms infrared (FTIR) spectroscopy of olive inflorescence flower anthesis

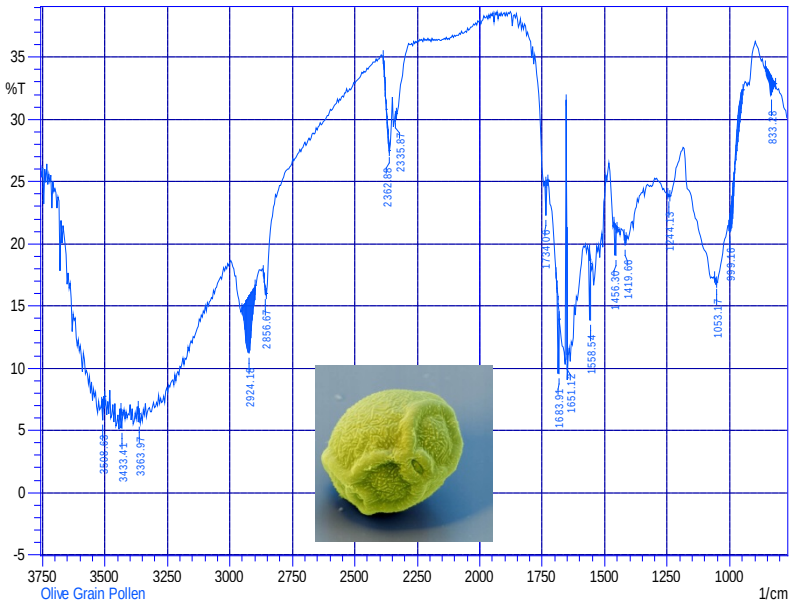

Fig. 10. Fourier transforms infrared (FTIR) spectroscopy of olive grain pollen

Inspection the results of the (Fig. 8, 9 and 10) indicates that the olive flower pre-anthesis, anthesis and grain pollen extracts contain oxygen and nitrogen atoms in functional groups (O–H, N–H, C=C, C=O, C=N, C–N, C–O) and aromatic ring, which meets the general consideration of typical corrosion inhibitors.

Table 6. Summary of the absorption bands for the olive flower pre-anthesis, anthesis and grain pollen extracts

Olive Inflorescence Flower Pre-Anthesis Extract	**Olive Inflorescence Flower Anthesis Extract**	**Olive Grain Pollen Extract**	**Stretching Vibration mode**
3564-3338	3398-3377	3500-3363	N-H or O-H(phenol)
2924	2928	2924	C–H
2854	2889	2856	C–H
2364	2360	2362-2335	C–H
-	1869	-	C–H
-	1734-1705	1734	C=O
1635	1635	1683	C=C and C=N
1618	-	1651	C=C and C=N
-	-	1558	C=C and C=N
1446	1437	1456-1419	C=C
-	1267	1244	C–H bending in –CH3
1074	1159-1076	1053	C–N or C–O (alcohol) or C–H

3.5. Explanation for inhibition

Olive flowers extracts are composed of numerous naturally occurring organic compounds. Accordingly, the inhibitive action of olive flower extracts could be attributed to the adsorption of its components on the steel surface.

4. CONCLUSION

Based on the results obtained from the weight loss methods and electrochemical measurements, the following conclusions are drawn:

- Olive flowers extracts (olive flower inflorescence pre anthesis, anthesis and grain pollen) act as a good corrosion inhibitor for C-steel in 1 M HCl solution.
- Inhibition efficiency (%IE) increases with the inhibitor concentration,
- The inhibition action of the extract was attributed to the physical adsorption of its compounds onto the steel surface.
- The extracts act as mixed inhibitors with significant cathodic efficiency. The inhibition efficiency values obtained from weight loss, polarization curves and EIS are in good agreement.
- The inhibition efficiency decreases with increasing temperature.
- Test results obtained from various corrosion techniques point out that the corrosion rate of mild steel increases with higher temperatures, which indicates that the adsorption of the extract on the metal surface is of the physiosorption type.
- The presence of extracts increases the activation energy of the corrosion process.
- The presence of extracts decreases the charge density in the transpassive region.
- The introduction of olive flower inflorescence pre anthesis, anthesis and grain pollen into HCl solution results in the formation of a film on the steel surface, which effectively protects steel from corrosion
- However, neither the molecular mechanism of the anti-corrosive nor the specific compound or mixture of compounds responsible for this bioactivity is known in detail.

Funding: This research did not receive any specific grant from funding agencies in the public, commercial, or not-for-profit sectors.

REFERENCES

[1] I. Merimi, Y. El Ouadi, K. R. Ansari, H. Oudda, B. Hammouti, and M. A. Quraishi, Anal. Bioanal. Electrochem. 9 (2017) 640.

[2] K. R. Ansari, and M. A. Quraishi, Anal. Bioanal. Electrochem. 8 (2016) 136.

[3] M. Galai, M. Rbaa, Y. El Kacimi, M. Ouakki, N. Dkhirech, R. Touir, B. Lakhrissi, and M. E. Touhami, Anal. Bioanal. Electrochem. 9 (2017) 80.

[4] C. Verma, M. A. Quraishi, and R. Korde, Anal. Bioanal. Electrochem. 8 (2016) 1012.
[5] N. K. Gupta, M. A. Quraishi, P. Singh, V. Srivastava, K. Srivastava, C. Verma, and A. K. Mukherjee, Anal. Bioanal. Electrochem. 9 (2017) 245.
[6] A. Fattah-Alhosseini, and B. Hamrahi, Anal. Bioanal. Electrochem. 8 (2016) 535.
[7] P. Dohare, D. S. Chauhan, B. Hammouti, and M. A. Quraishi, Anal. Bioanal. Electrochem. 9 (2017) 762.
[8] K. Alaoui, Y. El Kacimi, M. Galai, K. Dahmani, R. Touir, A. El Harfi, and M. Ebn Touhami, Anal. Bioanal. Electrochem. 8 (2016) 830.
[9] A. Benabida, M. Galai, M. Cherkaoui, and O. Dagdag, Anal. Bioanal. Electrochem. 8 (2016) 962.
[10] A. Fattah-Alhosseini, and M. Noori, Anal. Bioanal. Electrochem. 8 (2016) 145.
[11] L. Afia, R. Salghi, A. Zarrouk, H. Zarrok, E. H. Bazzi, B. Hammouti, and M. Zougagh, Trans. Indian Inst. Met. 66 (2013) 43.
[12] A. Bousskri, A. Anejjar, M. Messali, R. Salghi, O. Benali, Y. Karzazi, S. Jodeh, M. Zougagh, E. E. Ebenso, and B. Hammouti, J. Mol. Liq. 211 (2015) 1000.
[13] N. S. Patel, J. Hadlicka, P. Beranek, R. Salghi, H. Bouya, H. A. Ismat, and B. Hammouti,. Electrochim. Acta. 32 (2014) 395.
[14] L. Bammou, M. Belkhaouda, R. Salghi, O. Benali, A. Zarrouk, H. Zarrok, and B. Hammouti, J. Assoc. Arab Univ. Basic Appl. Sci. 16 (2014) 83.
[15] R. Salghi, L. Bazzi, B. Hammouti, S. Kertit, A. Bouchtart, and Z. El Alami, Ann. Chim. Sci. Matér. 25 (2000) 593.
[16] R. Salghi, L. Bazzi, and M. Zaafrani, Acta Chim. Slov. 50 (2003) 491.
[17] R. Salghi, M. Mihit, B. Hammouti, and L. Bazzi, J. Iran Chem. Res. 2 (2009) 157.
[18] A. Y. El-Etre, and A. I. Ali, Chin. J. Chem. Eng. 25 (2017) 373.
[19] D. S. Yang, H. X. Guo, J. X. Wang, (2007).
[20] R. Maillard, L'olivier. (1975) 24.
[21] L. Rallo, P. Torrefio, and A. Vargas, J. Acta Hortic. 356 (1994) 127.
[22] J. Cuevas, and V. S. Polito, Ann. Bot. 93 (2004) 547.
[23] S. Lavee, J. Taryan, J. Levin, and A. Haskal, Olivae 91 (2002) 25.
[24] A. Fabbri, and C. Benelli, J. Hortic. Sci. Biotechnol. 75 (2000) 131.
[25] G. C. Martin, J. H. Connell, M. W. Freeman, W. H. Krueger, and G. S. Sibbett, Acta Hortic. 356 (1994) 302.
[26] A. Díaz, and A. Martín, J. Am. Soc. Hort. Sci. 131 (2006) 250.
[27] E. S. El-hady, L. Haggag, F, M. M. M. Abd El-Migeed, and I. M. Desouky, Res. J. Agric. Biol. Sci. 3 (2007) 504.
[28] C. K. Kitsaki, E. Andreadis, and D. L. Bouranis, Flora 205 (2010) 599.
[29] K. Pinney, and V. S. Polito, Acta Hortic. 286 (1990) 203.

[30] I. Muzzalupo, Olive Germplasm - The Olive Cultivation, Table Olive and Olive Oil Industry in Italy, Published by InTech Janeza Trdine 9, 51000 Rijeka, Croatia,Chapter 2, (2012) 34.

[31] L. R. L. S. C. Ederli, and B. P. S. O. F. F. M. F. F. Romano, Sex Plant Reprod. 22 (2009) 109.

[32] A. Fabbri, G. Bartolini, M. Lambardi, S. Kailis, Olive Propagation Manual, ISBN: 9780643091016 , Publisher: Landlinks Press , (2004) pp. 9.

[33] A. Rosati, S. Caporali, A. Paoletti, and F. Famiani, Sci. Hortic. 127 (2011) 515.

[34] K. Uriu, Proc Amer. Soc. Hort. Sci. 73 (1960) 194.

[35] G. C. Martin, G. S. Sibbett, Oakland, California., in: Bot. Olive Sibbett GS Ferguson JL Coviello Lindstrand M Eds Olive Prod. Man. Univ. Calif. Agric. Nat. Resour. Oakl. Calif., (2005) pp. 15–19.

[36] L. Reale, C. Sgromo, T. Bonofiglio, F. Orlandi, F. Ferranti, and M. Fornaciari, Sex Plant Reprod. 19 (2006) 151.

[37] S. Lavee, L. Rallo, H. F. Rapoport, and A. Troncoso, Sci. Hortic. 66 (1996) 149.

[38] A. Rosati, M. Zipancic, S. Caporali, and A. Paoletti, Sci. Hortic. 126 (2010) 200.

[39] S. Wu, G. Collins, M. Sedgley, and J. Hortic. Sci. Biotechnol. 77 (2002) 665.

[40] M. I. Rodrîguez-Garîa, and M. D. C. Fernândez, Plant Syst. Evol. 171 (1990) 221.

[41] E. Pacini, New Phytol. 83 (1979) 157.

[42] M. D. Fernandez, and M. I. Rodriguez-garcia, Rev. Palaeobot. Palynol. 85 (1995) 99.

[43] M. I. Rodríguez-García, M. M'rani-Alaoui, and M. C. Fernández, Protoplasma 221 (2003) 237.

[44] A. Majewska-Sawka, M. C. Fernández, M. M'rani-Alaoui, A. Münster, and M. I. Rodríguez-García, Sex Plant Reprod. 15 (2002) 21.

[45] M. M. Altamura Betti, G. Pasqua, and G. Mazzolani, Ann. Bot. 40 (1982) 111.

[46] P. C. Martins, A. M. Cordeiro, and H. F. Rapoport, Adv. Hortic. Sci. 20 (2006) 262.

[47] A. Mazzeo, M. Palasciano, A. Gallotta, S. Camposeo, A. Pacifico, and G. Ferrara, Sci. Hortic. 170 (2014) 89.

[48] C. Galan, L. Vazquez, H. Garcıa-Mozo, and E. Field, Crops Res. 86 (2004) 43.

[49] J. Bousquet, B. Guerin, B. Hewitt, S. Lim, and F. B. Michel, Clin. Allergy 15 (1985) 439.

[50] F. Alagna, M. Cirilli, G. Galla, F. Carbone, L. Daddiego, P. Facella, L. Lopez, R. Colao, and C. Mariotti, PLoS ONE. 14 (2016) 1.

[51] L. Afia, R. Salghi, L. Bammou, L. Bazzi, B. Hammouti, and L. Bazzi, Acta Metall. Sin. Engl. Lett. 25 (2012) 10.

[52] M. Znini, M. Bouklah, L. Majidi, S. Kharchouf, A. Aouniti, A. Bouyanzer, and B. Hammouti, Int. J. Electrochem. Sci. 6 (2011) 691.

[53] P. Acevedo-Pena, and I. Gonzalez, J. Electrochem. Soc. 159 (2012) C101.

[54] R. Yadav, and P. S. Fedkiw, J. Electrochem. Soc. 159 (2012) B340.
[55] S. A. A. Yahia, L. Hamadou, A. Kadri, N. Benbrahim, and E. M. M. Sutter, J. Electrochem. Soc. 159 (2012) K83.
[56] A. Tebbji, K. Aouniti, B. Attayibat, A. Hammouti, A. Oudda,H. Benkaddour, M. Radi, and S. Nahle, Indian J. Chem. Technol. 18 (2011) 244.
[57] K. Tebbji, H. Oudda, B. Hammouti, M. Benkaddour, A. Aouniti, Radi, and S. Ramdani, A, Res. Chem. Intermed. 37 (2011) 985.
[58] A. Zarrouk, B. Hammouti, H. Zarrok, M. Al-Deyab, and S. S. Messali, Int. J. Electrochem. Sci. 6 (2011) 6261.
[59] E. R. Larios-Durán, and R. Antaño-López, J. Electroanal. Chem. 658 (2011) 10.
[60] H. Manjunatha, K. C. Mahesh, G. S. Suresh, and T. V. Venkatesha, Electrochim. Acta 56 (2011) 1439.
[61] S. A. Umoren, Y. Li, and F. H. Wang, J. Appl. Electrochem. 41 (2011) 307.
[62] F. Bentiss, C. Jama, B. Mernari, H. Attari, L. El-Kadi, M. Lebrini, M. Traisnel, and M. Lagrenée, Corros. Sci. 51 (2009) 1628.
[63] T. K. Dong, A. Kirchev, F. Mattera, J. Kowal, and Y. Bultel, J. Electrochem. Soc. 158 (2011) A326.
[64] A. Chetouani, B. Hammouti, T. Benhadda, and M. Daoudi, Appl. Surf. Sci. 249 (2005) 375.
[65] A. Chetouani, M. Daoudi, and B. Hammouti, Corros. Sci. 48 (2006) 2987.
[66] K. Laarej, M. Bouachrine, S. Radi, S. Kertit, and B. Hammouti, E-J. Chem. 7 (2010) 419.
[67] K. Barouni, L. Bazzi, R. Salghi, M. Mihit, B. Hammouti, S. Albourine, and A. El-Issami, Mater. Lett. J. 62 (2008) 3325.
[68] M. Bouklah, A. Attayibat, S. Kertit, A. Ramdani, and B. Hammouti, Appl. Surf. Sci. 242 (2005) 399.
[69] I. B. Obot, and N. O. Obi-Egbedi, Corros. Sci. 52 (2010) 198.
[70] M. Behpour, S. M. Ghoreishi, N. Mohammadi, N. Soltani, and M. Salavati-niasari, Corros. Sci. 52 (2010) 4046.
[71] N. Labjar, M. Lebrini, F. Bentiss, N.-E. Chihib, S. El Hajjaji, and C. Jama, Mater. Chem. Phys. 119 (2010) 330.
[72] M. Lebrini, M. Lagrenée, H. Vezin, M. Traisnel, and F. Bentiss, Corros. Sci. 49 (2007) 2254.
[73] X. Li, S. Deng, and H. Fu, Corros. Sci. 62 (2012) 163.
[74] A. R. S. Priya, V. S. Muralidharan, and A. Subramania, Corros. Eng. Sect. 64 (2008) 541.
[75] P. Bommersbach, C. Alemany-dumont, J. Millet, and B. Normand, Electrochim. Acta 51 (2006) 4011.

[76] C. H. Hsu, and F. Mansfeld, Corros. Sci. Sect. Tech. 57 (2001) 747.
[77] D. P. Schweinsberg, and V. Ashwortht, Corros. Sci. 28 (1988) 539.
[78] E. E. Oguzie, Corros. Sci. 50 (2008) 2993.
[79] M. Behpour, S. M. Ghoreishi, and N. Soltani, Corros. Sci. 51 (2009) 1073.
[80] X. Li, S. Deng, G. Mu, H. Fu, and F. Yang, Corros. Sci. 50 (2008) 420.